Adaptive configuration of generalized nonlinear ECM of Li-ion batteries based on impedance measurements and DRT analysis

1st Jussi Sihvo
Department of Electrical Engineering
Tampere University
Tampere, Finland
jussi.sihvo@tuni.fi

2nd Vaclav Knap
Department of Electrical Engineering
Czech Technical University in Prague
Prague, Czech Republic
vaclav.knap@cvut.cz

3rd Tomi Roinila
Department of Electrical Engineering
Tampere University
Tampere, Finland
tomi.roinila@tuni.fi

4th Daniel-Ioan Stroe
AAU Energy
Aalborg University
Aalborg, Denmark
dis@energy.aau.dk

***Index Terms*—Batteries, Battery electrochemical model, Battery impedance measurement, Battery Management Systems (BMS), State of charge.**

***Abstract*—An adaptive approach for configuration of generalized battery nonlinear equivalent-circuit-model (ECM) is proposed. In the approach, the distribution-relaxation-times (DRT) analysis is used to configure and initialize the ECM to be fitted to the impedance data. The performance of the approach is validated and analyzed by using experimental battery impedance measurements.**

I. Introduction

Li-ion batteries are becoming increasingly popular as an energy storage technology in electrification of energy and transportation sectors. Li-ion batteries are most often equipped with a battery-management-system (BMS) which monitors the battery and guarantees its safe operation. This is done by constantly monitoring the battery voltages, current and temperature. These measures are further used to determine state parameters, such as, state-of-charge (SOC) and state-of-health (SOH) which are important parameters in terms of safety and performance of the battery application. [1]

It is widely recognized that the battery impedance is an important measure in the estimation of SOC and SOH [2]–[4]. In addition, it is important parameter for dynamical simulations of battery systems and applications. The battery impedance can be measured by the electrochemical-impedance-spectroscopy (EIS) which produces complex-valued impedance data with frequency information [5]. In order to reduce the amount of data and to make its further use more feasible, the battery impedance can be mapped to equivalent-circuit-model (ECM) parameters. To model the non-linear shaping of the battery impedance, high amount of linear RC elements can be used [6], [7]. Alternative approach is to use nonlinear ECM in which a constant-phase-element (CPE) is typically used in parallel with a resistor to form a nonlinear RC element (also known as Zarc element) [8], [9]. In the case of using Zarc elements, an optimization algorithm, such as complex-nonlinear-least-squares (CNLS) algorithm, is used to fit the ECM accurately to the impedance data. In the dynamical analysis, the main objective is usually to obtain as accurate fit as possible which can be obtained with high amount of simple and linear RC elements. However, for the state estimation and observing applications, equally important objective is the parameter values and their trend evolution along the operating conditions to have a physical meaning. For these purposes, the nonlinear ECM approach over the linear approach is beneficial as the model parameters can be reduced and their physical interpretation simplified.

Many design phases in the nonlinear ECM approach affects on how the fitting objectives are reached. For example, the fitting algorithm and especially the selection of the initial conditions of the nonlinear ECM have significant effect on the fitting accuracy and also on the parameters' physical correlation [8]. In addition, the ECM should be selected and configured appropriately based on the shape of the impedance to guarantee the performance of the ECM approach. Typically, the research has been focused on specific case-studies of battery cells where the ECM is kept fixed at different operating condition (e.g. SOC, temperature, SOH, etc...) [6], [8], [9]. However, the shape of the impedance drastically changes along with the operating conditions which can lead to the ECM not being appropriate anymore. This significantly limits the ECM approach feasibility in realistic applications with changing operating conditions.

For the selection of the ECM, a distribution-of-relaxation-times (DRT) method has attracted research interest in recent

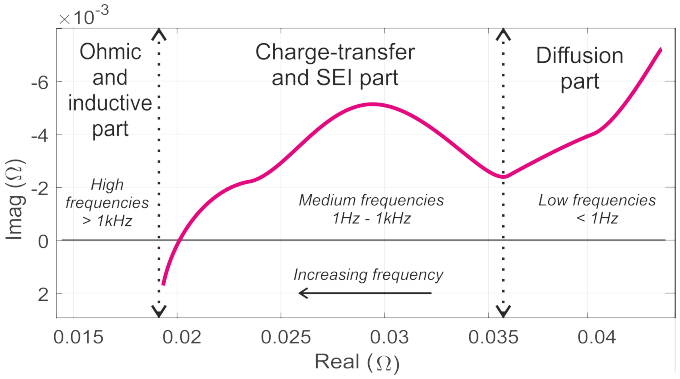

Fig. 1. Example plot of a battery impedance and its usual parts

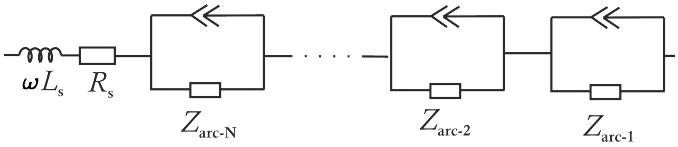

Fig. 2. Adaptively configurable nonlinear battery ECM used in the paper

years [7], [10], [11]. The DRT produces an estimate of the amount and values of existing time-constants (TC) of linear RC-elements in the impedance data, along with their relative magnitude in the impedance. The DRT analysis can, therefore, provide an adaptive estimate of the ECM configuration and parameterization from the measured impedance. The DRT has been demonstrated for obtaining the battery ECM approximated by linear RC-elements in [7], [11]. In the studies, the use of only a few linear RC elements is shown to be adequate enough for time-domain modeling but accurate frequency-domain modeling require extensive amount of RC-elements (10 or even more). With such high amount of circuit elements, many RC-elements together represents a single electrochemical process in the battery. This makes it hard to interpret which RC-elements are contributing to each process, and how many, and what kind of processes are generally active. The extension of the DRT method for nonlinear ECM approach would allow higher accuracy with significantly less circuit elements than that required for the linear ECM approach. Because of the reduced number of circuit elements and accurate fitting, the parameters are expected to have consistent behavior with physical correlation to the EIS data. It would also introduce the model itself being an extra parameter that can address how many and what electrochemical processes are contributing to the impedance. Such adaptive nonlinear ECM configuration and parameterization capabilities would be an effective tool for many types of practical battery applications.

This paper proposes an adaptive configuration of a generalized nonlinear ECM of a Li-ion battery impedance based on the DRT analysis applied to the EIS measurement data. In the method, The ECM is generalized by series resistor, inductor, and n-amount of parallel connected nonlinear elements given by the DRT analysis. The obtained ECM is furher adaptively parameterized based on both the DRT analysis and analytical methods. The proposed methods are validated by using experimental EIS data measured from a nickel-manganese-cobalt (NMC) Li-ion cell at various SOCs. It is shown that the method provides an accurate fit along with the parameters values and trends having good physical correlation with changing SOCs.

The rest of the paper is organized as follows: The theory of the adaptive ECM and the DRT method are presented in Sections II and III, respectively. The initialization and fitting of the ECM are presented in Section IV, and the experiments and results are presented in Sections V and VI, respectively. At last, the conclusions are drawn in Section VII.

II. Generalized ECM model

Fig. 1 shows a typical impedance of a Li-ion battery. The shape of the impedance can be considered to be formed of several different electrochemical processes of the cell. For the convenience, these processes can be divided into three parts: the diffusion part, the charge-transfer (CT)/solid-electrolyte-interface (SEI) part, and the ohmic and inductive part. These processes at these parts and their electrical dynamics are affected differently depending on the state of the battery. For example, the diffusion processes are highly affected as the SOC of the battery changes, while the CT/SEI processes are affected by both the SOC and SOH. In addition, the ohmic and inductive processes have high contribution to the SOH and for the capacity degradation in particular. [2], [3], [12]

The nonlinear ECM suitable for the adaptive selection is shown in Fig. 2. In the model, series resistance R_{s} and inductance ωL_{s} are used to model the ohmic and inductive part of the battery impedance. For the CT/SEI and diffusion processes, n-amount of Zarc elements are used which are comprised of a CPE and a resistor R_{arc} connected in parallel. The CPE consists of a generalized capacitance C and a suppression factor α as given in (1). Instead of capacitance, Zarc elements can be defined in terms of time-constant (TC) due to the relation $\tau^{\alpha} = RC$ as given in (2). This substitution is useful because of the further utilization of the DRT method.

Mathematical representation of the adaptive ECM is given in (3) where n is the total number of the Zarc elements with k running in a decreasing order of $\tau_{\text{arc-k}}$. Each Zarc element can be regarded to represent an electrochemical process in the battery, such as, solid-state diffusion in the diffusion part, and charge transfering and SEI at the CT/SEI part of the impedance [2], [13]. Each Zarc element has three parameters from which $\tau_{\text{arc-k}}$ represents the speed and $R_{\text{arc-k}}$ represents the dominance of the corresponding electrochemical process. Being an exponential term in (2), α is more difficult to be linked to an individual physical meaning. However, its role in the ECM parameterization is emphasized as it has significant effect on other parameter values and the fitting accuracy. Series parameters model the conductivity of electrical connection of the battery cell. Total number of the parameters in (3) equals $2+3n$. As the model is adaptively changing, n can be regarded

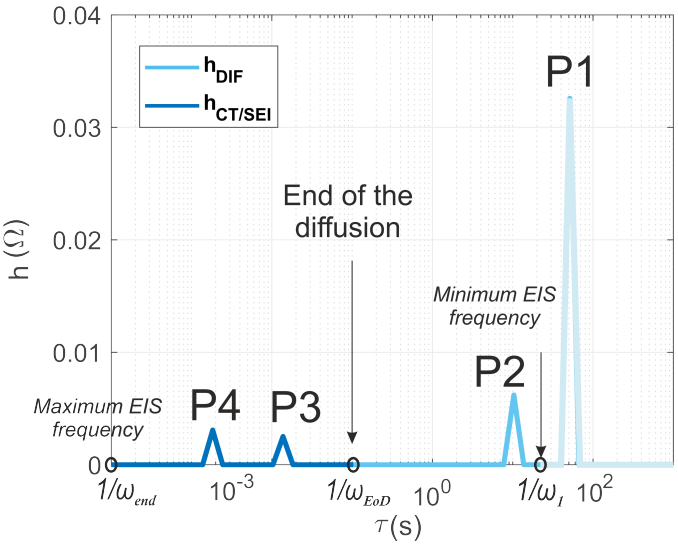

Fig. 3. Illustration of the time constants and boundary frequencies in the DRT spectra (corresponding to the EIS plot in Fig. 4)

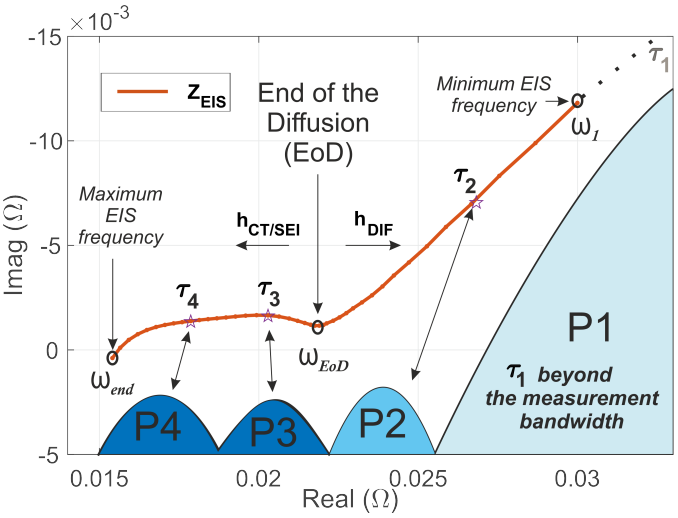

Fig. 4. Illustration of the time constants and boundary frequencies in the EIS spectra (corresponding to the DRT plot in Fig. 3)

as an extra parameter giving information about the number of processes contributing to the impedance.

$$Z_{\mathrm{CPE}}(j\omega) = \frac{1}{(j\omega)^{\alpha} C} \tag{1}$$

$$Z_{\text{arc-k}}(j\omega) = \frac{R_{\text{arc-k}}}{1 + (j\omega\tau_{\text{arc-k}})^{\alpha_{\text{arc-k}}}} \tag{2}$$

$$Z_{\mathrm{ECM}}(j\omega) = R_{\mathrm{s}} + j\omega L_{\mathrm{s}} + \sum_{k=1}^{n} Z_{\text{arc-k}}(j\omega) \tag{3}$$

III. DRT ANALYSIS

The DRT analysis aims to reveal what TCs are present in the observed data and what are their relative magnitudes with respect to each other. The DRT impedance can be defined as given in (4) which is comprised of a sum of linear RC-elements. In the equation, h_k includes the relative magnitude of the TCs τ_k and N is the number of TCs used for the analysis. Matching of the DRT impedance to the EIS data yields to a minimization problem given in (5) which can be solved with a linear least squares fitting algorithm.

$$Z_{\mathrm{DRT}} = \sum_{k=1}^{N} \frac{h_k}{1 + j\omega\tau_k} \tag{4}$$

$$J = ||\mathbf{A}\mathbf{x} - \mathbf{b}||^2 \tag{5}$$

$$\mathbf{x} = [h_1 h_2 ... h_N]^{\mathbf{T}} \tag{6}$$

$$\mathbf{b} = \begin{bmatrix} \mathrm{Re}\{Z_{\mathrm{EIS}}\} \\ \mathrm{Im}\{Z_{\mathrm{EIS}}\} \end{bmatrix} \tag{7}$$

$$\mathbf{A} = \begin{bmatrix} \mathrm{Re}\{\frac{1}{1+j\omega_1\tau_1}\} & \dots & \mathrm{Re}\{\frac{1}{1+j\omega_1\tau_N}\} \\ \vdots & \ddots & \vdots \\ \mathrm{Re}\{\frac{1}{1+j\omega_{N_\omega}\tau_1}\} & \dots & \mathrm{Re}\{\frac{1}{1j\omega_{N_\omega}\tau_N}\} \\ \mathrm{Im}\{\frac{1}{1+j\omega_1\tau_1}\} & \dots & \mathrm{Im}\{\frac{1}{1+j\omega_1\tau_N}\} \\ \vdots & \ddots & \vdots \\ \mathrm{Im}\{\frac{1}{1+j\omega_{N_\omega}\tau_1}\} & \dots & \mathrm{Im}\{\frac{1}{1j\omega_{N_\omega}\tau_N}\} \end{bmatrix}. \tag{8}$$

While being useful analyzing tool, the DRT method has some limitations that needs to be considered. The obtained DRT spectrum $\mathbf{x}$ depends highly on the DRT parameters which are mostly related to the linear least squares optimization algorithm that is required to solve (4). For example, the optimization algorithm must be forced to provide positive outputs to allow the results to be physically meaningful. In addition, the density of τ_k also has contribution to the obtained DRT spectra. It is suggested that the length of the TC vector should be an integer multiple of the amount of EIS data points [10]. By default, the DRT only applies for capacitive-resistive data and it cannot estimate inductive TCs from the data. While theoretically being able to estimate TCs that exceeds the bandwidth of the impedance harmonics, very long TCs with very high resistance can be difficult to be estimated. This mainly affects on the estimation reliability of the longest TC in the data dominating the diffusion part of the impedance. [10], [11]

Figs. 3 and 4 illustrate the DRT configurations applied in this paper. The DRT method is applied in two parts for the EIS data: separately for both the diffusion part and the CT/SEI part of the impedance. This is done in order to prevent the diffusion and CT/SEI parts from affecting each other especially in the proximity of the end-of-the-diffusion (EoD). The TC-vectors for the CT/SEI and diffusion parts are set to have two times the length of the EIS frequency vector between starting and ending angular frequencies of the corresponding part. As an exception, the diffusion part TC-vector is also extended beyond the lowest frequency harmonic ω_1 by two decades to increase the reliability on estimating the TC located in the proximity of $1/\omega_1$. Despite extended, only the TCs found in the range of $1/\omega_1 - 1/\omega_{\mathrm{end}}$ are considered for further analysis. In addition, adjacent TCs are added together in the analysis to reduce the amount of Zarc elements in (3).

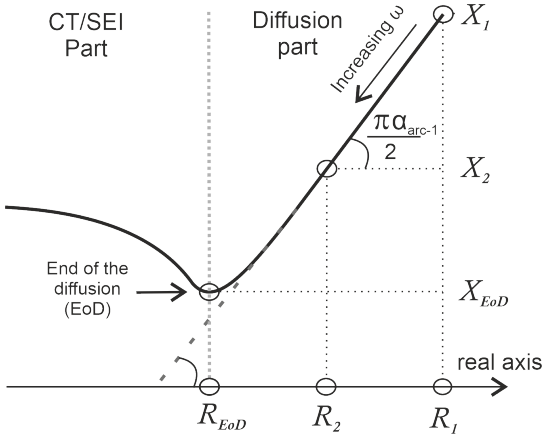

Fig. 5. Illustration of the initialization of $Z_{\text{arc-1}}$ parameters

This also gives good approximation for a group of linear RC-elements by one nonlinear Zarc element. After the analysis, the DRT magnitudes and TC vectors from the analysis are united as one single DRT magnitude and TC vectors as given in (9). The most dominating diffusion TC, being P1 in Fig 4, is not considered in the DRT analysis as it is found beyond the EIS bandwidth.

$$h_{\text{DRT}}(k) = \begin{bmatrix} h_{\text{DIF}}(k) \\ h_{\text{CT/SEI}}(k) \end{bmatrix}; \quad \tau_{\text{DRT}}(k) = \begin{bmatrix} \tau_{\text{DIF}}(k) \\ \tau_{\text{CT/SEI}}(k) \end{bmatrix} \tag{9}$$

IV. Initialization and fitting of the ECM

Once being configured by the DRT, the ECM parameters' initial conditions needs to be defined for the CNLS fitting. The initial conditions have a significant effect on the obtained fit and the parameter magnitudes. Care must be taken in order to initialize the parameters as close as possible to a physically meaningful solution. As the shape and magnitude of the battery impedance changes along operating conditions, also the initial conditions should be adaptively selected to guarantee similar baseline for every fitting of the EIS data. Analytical methods are used to initialize the series parameters and the Zarc element with the lowest TC ($Z_{\text{arc-1}}$) while the rest of the model parameters are initialized by the DRT analysis. It should be noted that the foregoing derivation is valid when the diffusion and CT/SEI parts are both included in the EIS bandwidth. [8]

The initialization can be started from the Zarc element with the longest TC in the diffusion part of the impedance ($Z_{\text{arc-1}}$) for which analytical methods are used for initialization. These methods are based on the work presented in [8] and are illustrated in Fig. 4. For obtaining the suppression factor, the diffusion part can be treated as a single CPE without the resistor and other circuit elements. In this case, the slope of the impedance determines α which can be calculated by using, for example, the first two data point of the measured impedance as given in (10). Furthermore, by separating imaginary part of (1), generalized capacitance can be obtained as given in (11).

$$\alpha_{\text{arc-1}} = \frac{2}{\pi}\text{atan}(\frac{X_1 - X_2}{R_1 - R_2}) \tag{10}$$

$$C_{\text{arc-1}} = -\frac{\sin(\frac{\pi\alpha_{\text{arc-1}}}{2})}{\omega_1^{\alpha_{\text{arc-1}}} X_1} \tag{11}$$

Obtained $\alpha_{\text{arc-1}}$ and $C_{\text{arc-1}}$ are now characterizing the CPE of $Z_{\text{arc-1}}$ which still needs the resistor to be initialized. This can be done by separating the real and imaginary part of (2) and by re-arranging either of them in terms of $R_{\text{arc-1}}$ as given in (12) for the real-part. $R_{\text{arc-1}}$ can be solved by applying quadratic equation to (13) from which the positive solution should be selected. At last, the required TC can be obtained from the relation given in (14).

$$aR_{\text{arc-1}}^2 + bR_{\text{arc-1}} + c = 0$$

$$\begin{aligned} a &= (R_1 - R_{\text{EoD}})\omega_1^{2\alpha_{\text{arc-1}}} C_{\text{arc-1}}^2 - \cos(\frac{\pi\alpha_{\text{arc-1}}}{2})\omega_1^{\alpha_{\text{arc-1}}} C_{\text{arc-1}} \\ b &= 2(R_1 - R_{\text{EoD}})\cos(\frac{\pi\alpha_{\text{arc-1}}}{2})C_{\text{arc-1}}\omega_1^{\alpha_{\text{arc-1}}} - 1 \\ c &= R_1 - R_{\text{EoD}} \end{aligned} \tag{12}$$

$$R_{\text{arc-1}} = \frac{-b \pm \sqrt{b^2 - 4ac}}{2a} \tag{13}$$

$$\tau_{\text{arc-1}} = (C_{\text{arc-1}} R_{\text{arc-1}})^{\frac{1}{\alpha_{\text{arc-1}}}} \tag{14}$$

For the initialization of the rest of the Zarc elements, either located at the diffusion or the CT/SEI part, the DRT analysis can be effectively generalized. As the relative DRT magnitudes can be considered to be valid, it is possible to scale them to make also the absolute values to adapt to the impedance data. For the scaling of the DRT magnitudes, the width of the CT/SEI part is useful for two reasons. At first, there should be one or more TCs located within that part, and second, its end points Zend and Z_{EoD} have low capacitive impedance [6]. Thus, any TCs in the impedance have minimal effect at these points which gives certainty for the scaling. The scaling factor C_{coeff} can be defined from (15) where R_{EoD} and R_{end} are the real part of the impedance at EoD and at the highest frequency harmonic, and o is the number of found TC in the CT/SEI part. C_{coeff} can also be used for scaling of h_{DIF}. Therefore, $R_{\text{arc-k}}$ can generally be obtained as given in (16) where n is the total amount of Zarc elements. $\tau_{\text{arc-k}}$ are directly accessible from t_{DRT} as given in (17).

$$C_{\text{coeff}} = \frac{R_{\text{EoD}} - R_{\text{end}}}{\sum_{k=1}^{o} h_{\text{CT/SEI}}(k)} \tag{15}$$

$$R_{\text{arc-k}} = C_{\text{coeff}} h_{\text{DRT}}(k) \tag{16}$$

$$\tau_{\text{arc-k}} = \tau_{\text{DRT}}(k), \qquad k = 2, 3, .., n \tag{17}$$

$$\alpha_{\text{arc-k}} = \frac{4}{\pi}\text{atan}(\frac{1}{C_{\text{coeff}}}). \tag{18}$$

For a single ideal Zarc element, suppression factor can be accurately obtained from the relation of the impedance imaginary- and real parts at frequency $\omega^\alpha = \frac{1}{RC}$. Despite being able to obtain ω accurately from the DRT analysis, the

effect of other Zarc elements at that frequency distorts that relation - making the approach highly uncertain. A method utilized here is to approximate the relation in [8] as the inverse of the scaling factor C_{coeff} with which $\alpha_{\text{arc-k}}$ can be obtained as given in (18). With this approach, α will be the same for each $Z_{\text{arc-k}}$ when $k = 2, .., n$.

At last, the series elements R_{s} and L_{s} can be obtained by utilizing the last frequency ω_{end} in the measurements. As all other elements are now obtained, R_{s}, can be solved from the real part and L_{s} from the imaginary part of (3) as given in (19) and (20), respectively.

$$R_{\text{s}} = \text{Re}\{Z_{\text{EIS}}(j\omega_{\text{end}})\} - \sum_{k=1}^{n} \text{Re}\{Z_{\text{arc-k}}(j\omega_{\text{end}})\} \tag{19}$$

$$L_{\text{s}} = \frac{\text{Im}\{Z_{\text{EIS}}(j\omega_{\text{end}})\} - \sum_{k=1}^{n} \text{Im}\{Z_{\text{arc-k}}(j\omega_{\text{end}})\}}{j\omega_{\text{end}}} \tag{20}$$

V. Experiments

The performance of the proposed techniques are demonstrated for battery EIS measurements carried out to a NMC-cell. The cell is discharged in a controlled environment at a constant temperature of 25 degrees of Celsius with EIS measured between 100% - 0% of SOC with 20% SOC resolution. The EIS measurement are carried out with a commercial battery spectrum analyzer with 45 logarithmically-spaced frequency harmonics divided between 10mHz and 3kHz.

The EIS data are applied to (4) - (9) to adaptively configure the nonlinear ECM while its parameters are initialized are obtained from (10) - (20). The fitting is carried out with a CNLS algorithm in MATLAB by *lsqcurvefit* -function. During the fitting, each suppression factor is treated as a constant in order to minimize their dominance to other model parameters. The goodness of the obtained fits are analyzed in terms of normalized-root-mean-square-error (NRMSE) given in (21) where l is the number of EIS harmonics and Z_{fit} is the fitted impedance. The normalizing factor in the denominator is absolute maximum difference in the measured impedance.

$$\text{NRMSE} = \frac{\sqrt{\frac{1}{l}\sum_{i=1}^{l}(1 - \frac{||Z_{\text{fit}}(i)||}{||Z_{\text{EIS}}(i)||})^2}}{\max(||Z_{\text{EIS}}||) - \min(||Z_{\text{EIS}}||)} \tag{21}$$

VI. Results

Fig. 6 shows raw EIS data from the measurements at different SOC values. The impedances are mostly varying at 0% and 100% of SOC while at medium SOCs they are very similar. Fig. 7 shows an example of the initial conditions and fitting results of the impedance measured at 60% of SOC. NRMSE errors for the fits are generally below 0.3%, as shown in Table I, which are highly accurate. The impedance obtained with the initial conditions have errors between 2-6% which provide a good baseline for the CNLS to converge consistently. At 100% of SOC, the ECM was configured to have three Zarc elements, whereas other measurements were configured to have four as can be seen from Table I. Fig. 8 shows the DRT plots of selected measurements from which it can be seen

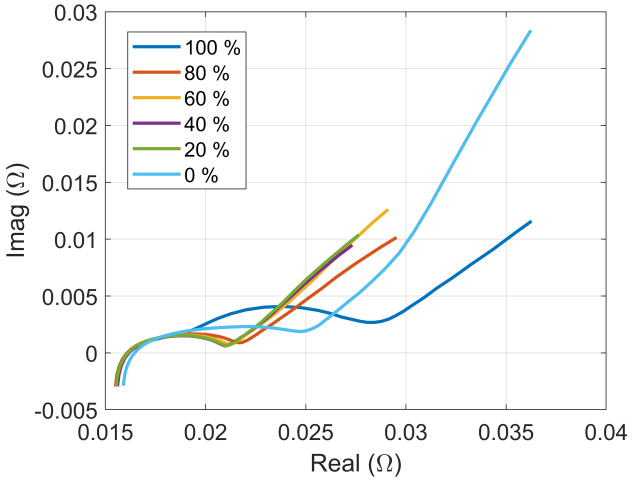

Fig. 6. EIS-measured battery impedances at various SOCs

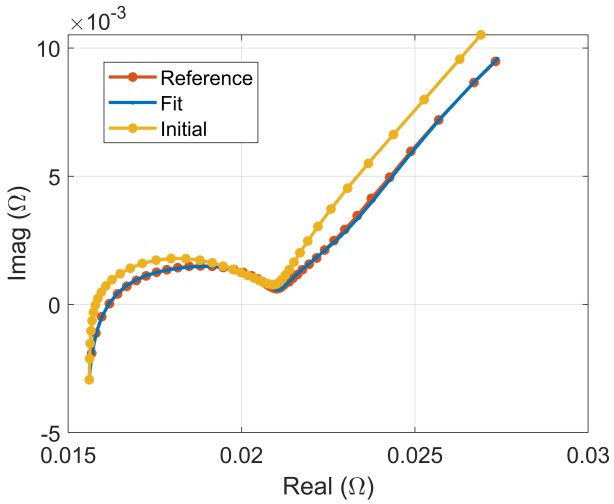

Fig. 7. Comparison of EIS-measured, initialized and fitted impedances at 60% of SOC

that the measurement at 100% of SOC has two peaks while other plots have three. It can be seen that this peak is missing at the diffusion part of the impedance. It should be noted that the number of peaks in Fig. 8 is one less than the numbers in Table I as the first Zarc element is not initialized by the DRT analysis.

Fig. 9 shows the magnitude of the fitted and initialized parameters and their trends along the SOC. The magnitudes and trends of the parameters can be analyzed by using two

TABLE I
NRMSE values and number of configured Zarc elements used in the ECM

SOC	**0%**	**20%**	**40%**	**60%**	**80%**	**100%**
Fit err	0.28%	0.26%	0.24%	0.30%	0.22%	0.19%
Init. err	2.28%	4.35%	4.65%	5.94%	5.37%	4.20%
Zarc elements (n)	4	4	4	4	4	3

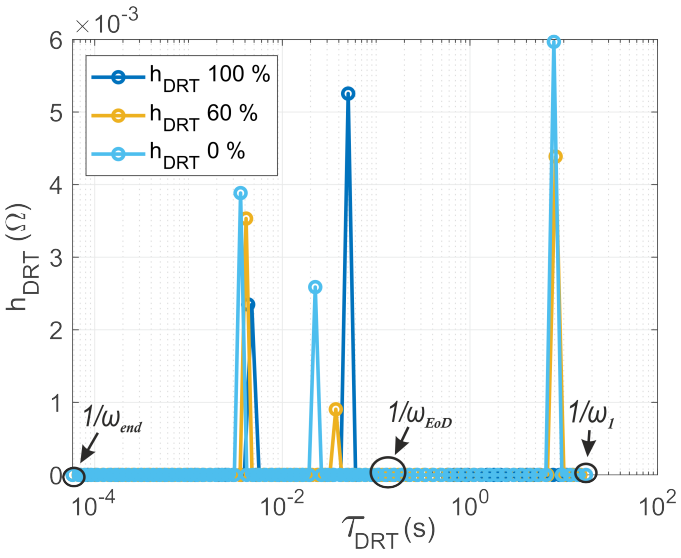

Fig. 8. DRT spectrum of measurements obtained at various SOCs

validation benchmarks. At first, the series resistance should equal the real-part offset from the origin, i.e. the minimum real part of the EIS plots. In addition, the sum of the CT/SEI part resistances should equal the width of the CT/SEI part in the EIS plot. By comparing the values to the EIS plots in Fig. 6, it can be concluded that these benchmarks are well satisfied. Thus, the parameter magnitudes can be regarded to have good physical correlation to the EIS data. The trends of the resistance values are also very similar to the EIS plots by showing no significant changes between 20-80% of SOCs. The trends of the fitted and initialized parameters are also very similar which tells about the consistency of the proposed methods. The foregoing analysis gives credibility also for the validity of $\tau_{\text{arc-k}}$ and L_s. For the suppression factors, values between 0.5-1 with no significant changes are considered sufficient as they are required only to guarantee stability and consistency of other ECM parameters. Based on the percentual errors, visual evidence and parameter magnitudes, it can be concluded that the presented methods are able to configure and parameterize the ECM accurately, adaptively and consistently.

VII. Conclusions

In this paper, an adaptive approach for configuration and parametrization of the battery nonlinear ECM has been proposed. The approach is based on the distribution-relaxation-times (DRT) analysis which produces an estimate of the number and values of the time constant. The DRT analysis is used to select suitable ECM for the measured impedance data and to initialize the parameters for the fitting algorithm. The performance of the approach is validated for impedance measured from a Li-ion NMC cell at various SOCs. The results showed that the adaptive approach is able to find suitable ECM and accurately fit it to the impedance data. In addition, the performance is consistent and the both the magnitudes and trends of the fitted parameters are shown to have good

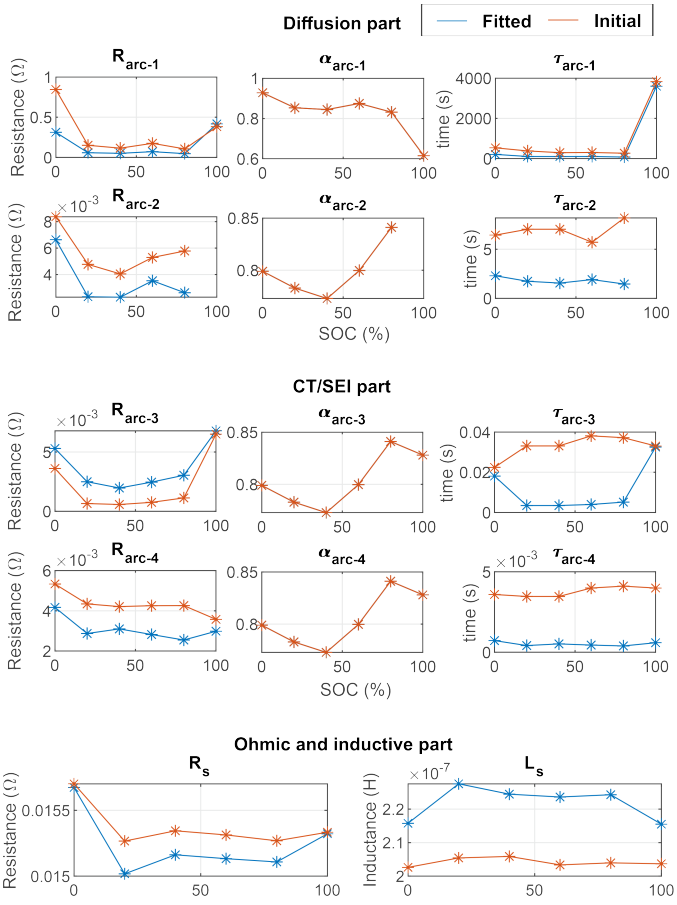

Fig. 9. ECM parameters as a function of SOC

physical correlation to the impedance data. Thus, the proposed methods provides a generic ECM modeling technique which is suitable for both dynamical analysis and state estimation of Li-ion batteries and applications.

References

[1] Y. Wu, *Lithium-Ion Batteries Fundamentals and Applications*. CRC Press, 2015.

[2] C. Pastor-Fernández *et al.*, "A comparison between electrochemical impedance spectroscopy and incremental capacity-differential voltage as li-ion diagnostic techniques to identify and quantify the effects of degradation modes within battery management systems," *Journal of Power Sources*, vol. 360, pp. 301–318, 2017.

[3] M. Petzl, M. Kasper, and M. A. Danzer, "Lithium plating in a commercial lithium-ion battery – a low-temperature aging study," *Journal of Power Sources*, vol. 275, pp. 799–807, 2015.

[4] M. A. Hannan, M. S. Lipu, A. Hussain, and A. Mohamed, "A review of lithium-ion battery state of charge estimation and management system in electric vehicle applications: Challenges and recommendations," *Renewable and Sustainable Energy Reviews*, vol. 78, pp. 834–854, 2017.

[5] A. Barai, G. H. Chouchelamane, Y. Guo, A. McGordon, and P. Jennings, "A study on the impact of lithium-ion cell relaxation on electrochemical impedance spectroscopy," *Journal of Power Sources*, vol. 280, pp. 74–80, 2015.

[6] A. Farmann, W. Waag, and D. U. Sauer, "Adaptive approach for on-board impedance parameters and voltage estimation of lithium-ion batteries in electric vehicles," *Journal of Power Sources*, vol. 299, pp. 176–188, 2015.

[7] J. P. Schmidt, P. Berg, M. Schönleber, A. Weber, and E. Ivers-Tiffée, "The distribution of relaxation times as basis for generalized time-domain models for li-ion batteries," *Journal of Power Sources*, vol. 221, pp. 70–77, 2013.

[8] J. Sihvo, T. Roinila, and D.-I. Stroe, "Novel fitting algorithm for parametrization of equivalent circuit model of li-ion battery from broadband impedance measurements," *IEEE Transactions on Industrial Electronics*, vol. 68, no. 6, pp. 4916–4926, 2021.

[9] P. Vyroubal and T. Kazda, "Equivalent circuit model parameters extraction for lithium ion batteries using electrochemical impedance spectroscopy," vol. 15, 2018, pp. 23–31.

[10] M. A. Danzer, "Generalized distribution of relaxation times analysis for the characterization of impedance spectra," *Batteries*, vol. 5, no. 3, 2019.

[11] L. Wildfeuer, P. Gieler, and A. Karger, "Combining the distribution of relaxation times from eis and time-domain data for parameterizing equivalent circuit models of lithium-ion batteries," *Batteries*, vol. 7, no. 3, 2021.

[12] J. Sihvo, T. Roinila, and D.-I. Stroe, ""soh analysis of li-ion battery based on ecm parameters and broadband impedance measurements," iecon 2020 the 46th annual conference of the ieee industrial electronics society, pp. 1923-1928,," 2020.

[13] E. Goldammer and J. Kowal, "Determination of the distribution of relaxation times by means of pulse evaluation for offline and online diagnosis of lithium-ion batteries," *Batteries*, vol. 7, no. 2, 2021.